Does trace element composition of bivalve shells record utra-high frequency environmental variations?

Pierre Poitevin, Laurent Chauvaud, Christophe Pécheyran, Pascal Lazure, Aurelie Jolivet, Julien Thébault

Does trace element composition of bivalve shells record utra-high frequency environmental variations?

Pierre Poitevin[*1, 2], Laurent Chauvaud[1], Christophe Pécheyran[3], Pascal Lazure[4], Aurélie Jolivet[5], Julien Thébault[1]

[1] *Univ. Brest, CNRS, IRD, Ifremer, LEMAR, F-29280 Plouzané, France*

[2] *Fisheries and Oceans Canada, Maurice Lamontagne Institute, Mont-Joli, QC, Canada*[3] *Laboratoire de Chimie Analytique Bio-inorganique et Environnement, Institut Pluridisciplinaire de Recherche sur l'Environnement et les Matériaux, CNRS, UMR 5254, Université de Pau et des Pays de l'Adour, Pau, France*[4] *Univ. Brest, CNRS, IRD, UBO, Ifremer, LOPS, F-29280 Plouzané, France*

[5] *TBM environnement/Somme, 2 rue de Suéde, 56400 Auray, France*

Email addresses:

Pierre Poitevin: poitevin.pierre@gmail.com

Laurent Chauvaud: laurent.chauvaud@univ-brest.fr

Christophe Pécheyran: christophe.pecheyran@univ-pau.fr

Pascal Lazure: pascal.lazure@ifremer.fr

Aurélie Jolivet: a.jolivet@tbm-environnement.com

Julien Thébault: julien.thebault@univ-brest.fr

Corresponding author:

Pierre Poitevin

Université de Bretagne Occidentale

Institut Universitaire Européen de la Mer

Laboratoire des Sciences de l'Environnement Marin (UMR6539 UBO/CNRS/IRD/Ifremer)

F-29280 Plouzané

Tel: +33 2 90 91 55 78

Fax: +33 2 98 49 86 45

Abstract

Saint-Pierre and Miquelon (SPM) is a small archipelago where instrumental measures based on water column velocity and temperature profiles compiled comprehensive evidence for strong near-diurnal (25.8h) current and bottom temperature oscillations (up to 11.5°C) which is possibly the largest ever observed — at any frequency — on a stratified mid-latitude continental shelf. The main objective of our study was to identify if *Placopecten magellanicus* can record on its shell these high frequency environmental variations. To this end, we have tried to identify proxies for water temperature and food availability through development of a new ultra-high resolution LA-ICPMS analyses method capable of resolving shell surface elemental composition with a 10 µm resolution. This method was applied on two shell fragments, both representing the third year of growth and 2015 annual growth period, respectively coming from two environmentally contrasted sites, more (30 m depth) or less (10 m depth) affected by high frequency thermal oscillations. Our results strongly suggest a relationship between phytoplankton biomass and barium incorporation into *P. magellanicus* shells at both sites. Even if *P. magellanicus* might present a physiological control of magnesium incorporation, the shape of the two Mg/Ca profiles seems to illustrate that temperature also exerts a control on magnesium incorporation in *P. magellanicus* shells from SPM. While U/Ca and Mg/Ca profiles show a strong positive correlation for 30 m site shell, suggesting that uranium incorporation in *P. magellanicus* shell is at least partially temperature dependent. The absence of such correlation for 10 m site shell suggests differences in uranium environmental availability or in *P. magellanicus* biomineralization between these two sites. The resolution of this new analytical method raises questions about such data interpretation related to *P. magellanicus* growth dynamics and physiology or individual scale based environmental measurements.

Keywords: Ultra-high resolution LA-ICPMS; *Placopecten magellanicus*; shell chemistry; trace elements; environmental change; bivalve; environmental proxies; North Atlantic; Saint-Pierre and Miquelon; Coastal Trapped Wave.

1. Introduction

Saint-Pierre and Miquelon (SPM) is a small archipelago at the confluence of major oceanic currents, marking the boundary between the North Atlantic Ocean subtropical and subpolar gyres. However, SPM archipelago hydrodynamics is poorly known and its physic observations (sensor deployments) only began very recently. In this context, instrumental measurements based on water column velocity and temperature profiles compiled comprehensive evidence for strong near-diurnal (25.8h) current and bottom temperature oscillations (up to 11.5°C) from July to October between 10 and 80m depth. This feature is possibly the largest ever observed, at any frequency, on a stratified mid-latitude continental shelf (Lazure *et al*., 2018). The extremely unstable physical nature of this sub-tidal environment associated with the presence of poikilothermic organisms represents a true ecological paradox, making this site a relevant place to study benthic organism responses to chronic thermal variations.

Biogenic carbonate with recognizable periodic growth bands, such as bivalve molluscs can incorporate minor and trace elements into their shells, in amounts depending on their concentrations in the environment and on the physical and biological properties of the surrounding seawater. However, bivalve shell biomineralization is a complex process, subject to strong physiological and kinetic effects related to metabolism, growth rates, ontogenetic age, shell mineralogy, crystal fabrics and organic matrix (e.g. Carré *et al.*, 2006; Freitas *et al.*, 2008; Freitas *et al.*, 2009; Freitas *et al.*, 2016; Klein *et al*., 1996; Lazareth *et al.*, 2013; Lorens and Bender, 1977; Schöne *et al*., 2013; Shirai *et al.*, 2014). Owing to their wide geographic distribution, economic importance, rapid growth rates, and the presence of annual growth lines on their shell, pectinid bivalves (aka. scallops) offer good opportunities to document past environmental conditions (Chauvaud *et al.*, 1998). The occurrence of a clearly visible annual banding pattern on the upper valve of the Atlantic sea scallop, *Placopecten magellanicus*, and the presence of this species in SPM over a wide bathymetric gradient (5 to 80 m), make this species a good candidate to track high-frequency past environmental changes - reflected as variations in the shell geochemical properties – at extremely high temporal resolution.

Spatially-resolved geochemical analysis of biogenic carbonates deposited between two accurately dated growth lines can be performed with a wide set of methods, such as laser ablation inductively coupled mass spectrometry (LA-ICPMS), secondary ion mass spectrometry (nanoSIMS) or electron micro probe analyser (EMPA). Because of its potential

for rapid and accurate high-resolution *in situ* trace element analysis at relatively low cost and minimal sample preparation requirements, LA-ICPMS has become a routine analytical tool in a wide area of research applications (Warter and Müller, 2017).

As bivalve growth rates have often been related to environmental variables such as food availability or water temperature (Ballesta-Artero *et al.*, 2017; Butler *et al.*, 2010; Marali and Schöne, 2015; Witbaard *et al.*, 1997) and because of the importance of these two parameters to track environmental and ecological changes, we then understand the interest to track and calibrate elemental proxy records of these two variables. For example, some authors proposed that magnesium to calcium ratios (Mg/Ca) can be used to record water temperature (Ullmann *et al.,* 2013, Bougeois *et al.,* 2014), while there are many reports of strong vital effects in bivalve shells for this element (Lorrain *et al.,* 2005, Wanamaker *et al.*, 2008, Surge and Lohmann, 2008). Uranium-to-calcium ratio has also been suggested as a proxy for temperature in shallow-water corals (Min *et al.,* 1995; Shen and Dunbar, 1995) and in planktonic foraminiferal carbonates (Yu *et al.*, 2008). Some authors also found a pH effect on U/Ca ratios in both inorganic aragonite and calcite (Kitano and Oomori, 1971; Chung and Swart, 1990). Indeed, U/Ca ratios in calcium carbonate are negatively correlated with pH and $[CO_3^{2-}]$, because in aqueous solutions the carbonate ion complexes with the uranyl ion (UO_2^{2+}) at higher pH (Langmuir, 1978), therefore less uranium is available to be incorporated in shell carbonate. Regarding U/Ca ratio on mollusc shells, Frieder *et al.* (2014) demonstrated that U/Ca varies as a function of pH in shells of living larvae in *Mytilus californianus* and *Mytilus galloprovincialis*. More recently, Zhao *et al.* (2018) demonstrated by measuring U/Ca ratio on *Mya arenaria* shells exposed to pCO_2-enriched environments the existence of efficient regulatory mechanisms to tightly control the pH at the site of calcification of this species. . Ba/Ca profiles in bivalve shells are typically characterized by a flat background signal interrupted by sharp peaks. Background level has been suggested to be linked with salinity (Gillikin *et al.*, 2006, 2008). As for peaks, many authors suggested a synchronization with phytoplankton blooms (e.g. Elliot *et al*., 2009; Lazareth *et al*., 2003; Stecher *et al*., 1996; Thébault *et al*., 2009; Vander Putten *et al.*, 2000). Building on the work of Stecher and Kogut (1999), Thébault *et al*. (2009) proposed two main hypotheses to explain the peaks: (1) ingestion of barite originating from assemblages of recently dead diatoms or (2) adsorption of barium onto iron oxyhydroxides associated with diatoms frustules.

The main objective of our study was to identify whether the calcitic shell of *P. magellanicus* can record the high frequency (25.8 h) environmental variations observed in SPM. To this end, we have developed a new ultra-high resolution LA-ICPMS analytical method in order to investigate skeletal trace element concentration with a 10 µm resolution. Results of our investigation can contribute to a better understanding of environmental and physiological mechanisms associated to sub daily environmental variations on ions incorporation into fast growing marine bivalve shells.

2. Materials and Methods

2.1 Sample collection

Two live *P. magellanicus* were collected in September 2016 from Saint-Pierre Bay (Saint-Pierre and Miquelon – NW Atlantic) respectively at 10 m and 30 m depth (Figure 1). Both individuals were in their fourth year of growth. The deepest location consisted in a homogeneous substrate, made of compacted and stable fine sand. At the shallowest one, the substrate was more heterogeneous and consisted of a mixture of gravels, pebbles, and rocks with a seaweed cover. Soft tissues were removed immediately after collection. Both shells were carefully cleaned with freshwater to remove adherent sediment and biological tissues before sample preparation.

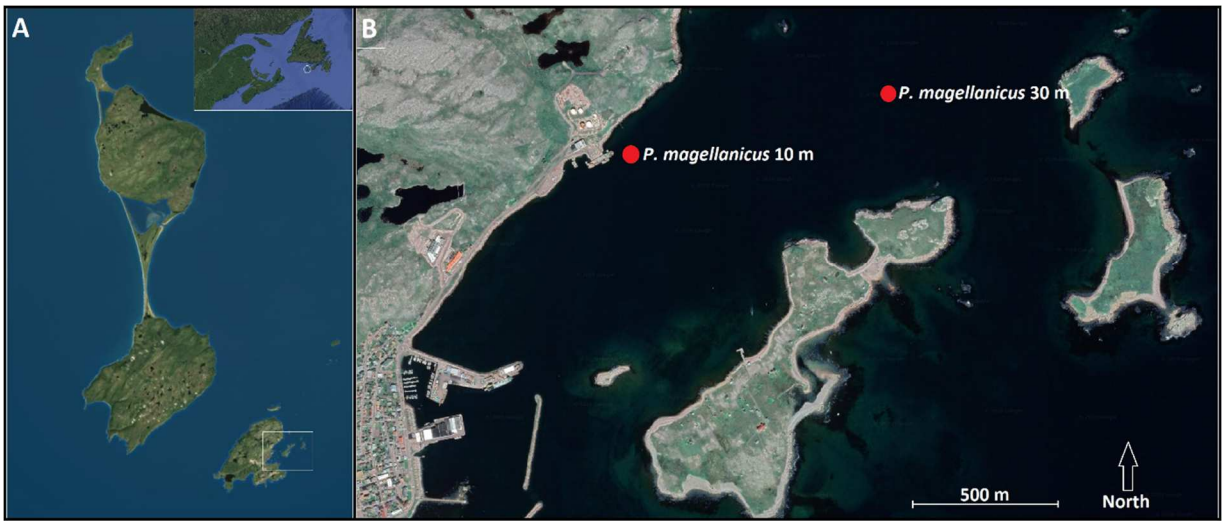

Figure 1: (A) Location of Saint-Pierre and Miquelon archipelago. (B) Satellite image of *P. magellanicus* sampling sites (red dots) in Saint-Pierre Bay.

2.2 Environmental monitoring

Annual thermal profiles at 10 m and 30 m discussed were derived from Lazure *et al.* (2018) study. To refine our vision of thermal variations on the two collection sites (Figure 1), three multi-parameter probes measuring temperature every 5 minutes were deployed at 8 m, 12 m and 30 m depth, between 28/08/2017 and 15/09/2017. The 2015 monthly satellite chlorophyll *a* measurements were downloaded from the GlobColour website (http://hermes.acri.fr) and are weighted monthly averages of single-sensor products (SeaWiFS/MERIS/MODIS/VIIRSN merged chlorophyll concentrations) over the area 46.6–47.3°N / 56.0–56.6°W (i.e., waters surrounding the SPM archipelago within ca. 30 km).

2.3 Sample preparation

All micro-chemical analyses were performed on *P. magellanicus* upper valves. Indeed, the lower valves might have been contaminated as a result of a prolonged contact with the sediment. For each individual, a fragment of shell of *ca.* 3.5 cm x 1 cm was cut with a diamond saw, including the axis of maximal growth (Figure 2).

Figure 2: Example of one *P. magellanicus* fragment used for LA-ICPMS analyses. White arrows indicate annual shell growth lines positions defining 2015 increment.

All ultra-high resolution LA-ICPMS analyses were performed one these two shell portions. These fragments represent, for each individual, the third year of growth corresponding to 2015 annual growth periods. The outer shell layer was ultrasonically cleaned with deionized water to remove organic matter and sediment particles. In addition, before LA-ICPMS analyses, the outer shell layer of each sample was chemically cleaned with a 15 seconds acetic acid (10 %) bath, soaked in deionized water during 10 seconds, and left to air dry in the LA-ICPMS clean room.

2.4 Ultra-high resolution fs-LA-ICPMS analysis

A UV high-repetition-rate femtosecond laser ablation (fs-LA) system (Nexeya SA, Canejan, France) was employed (Pulse duration: 360fs; wavelength: 257 nm). Each ICPMS measurement point represents an ablation transect with a 1-mm long arcuate trajectory, parallel to the ventral margin, made by fast round trips of a 10 µm spot (Figure 3). All transects were adjacent in order to analyse the whole "2015 annual period of growth" for the two individuals. The area, covered by a 1 mm x 10 µm transect is equivalent to the area covered by a 110 µm diameter round spot.

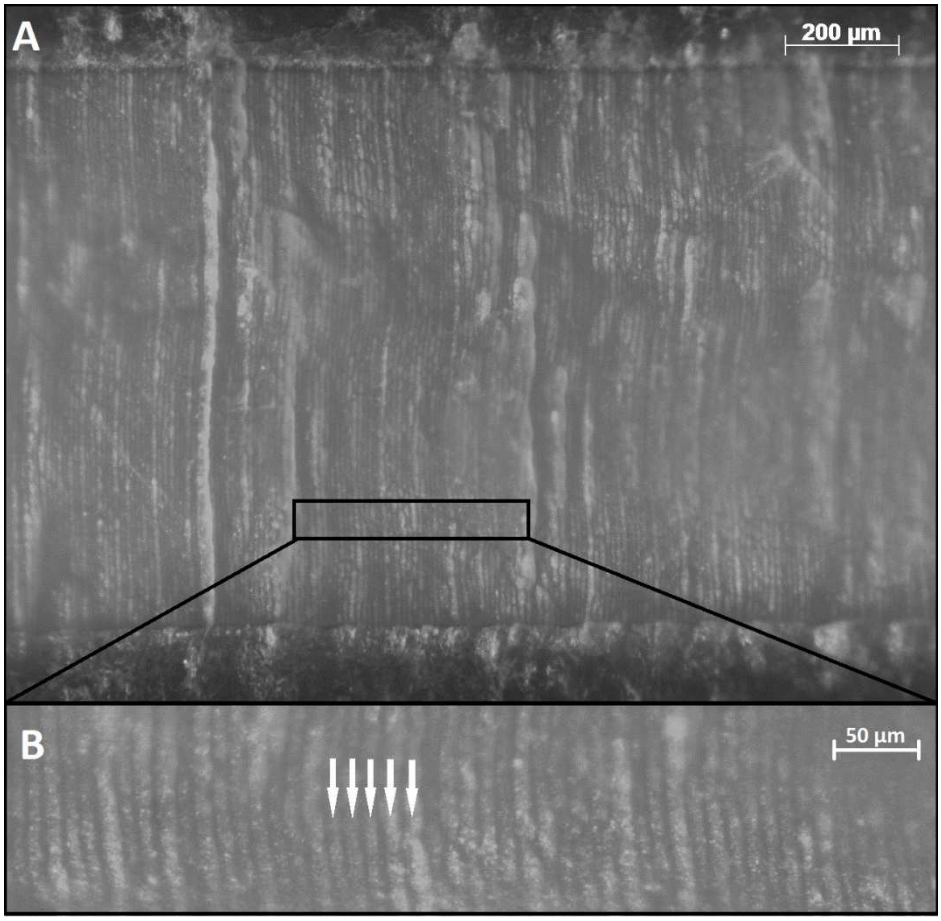

Figure 3: Post ablation picture of a 1.5 mm *P. magellanicus* section showing ca. 150 femtosecond laser ablation transects (A). Zoom on a small fraction of them, each white arrow points to a laser ablation transect (B). The visible lines represent ridges generated during the laser ablation process.

Outer shell layers were analysed for Mg/Ca, Ba/Ca and U/Ca ratios using a high-resolution inductively coupled plasma mass spectrometer fitted with a jet interface (Element XR, Thermo

Scientific, USA). A helium gas stream carried ablated material to the HR-ICP-MS (carrier gas flow rate 0.68 $L.min^{-1}$). Elemental ratios were quantified by monitoring ^{43}Ca, ^{24}Mg, ^{138}Ba, and ^{238}U. Calcium was used as an internal standard. Elements were standardized to calcium based on the stoichiometry of calcium carbonate (388 000 $\mu gCa.g^{-1}$ outer shell layer), assuming 100 % $CaCO_3$: Mg/Ca ($\mu g.g^{-1}$), Ba/Ca ($\mu g.g^{-1}$) and U/Ca ($\mu g.g^{-1}$). Quantification of trace elements in otoliths was achieved by external calibration using both carbonate pellets FEBS-1 (Barats et al., 2007) and 2 NIST glass standards (610, 612) to ensure the best accuracy. Each standard was analysed three times before and after each session with the laser to account for drifting during the day. The limits of detection (µg.g-1 in shells) achieved in this study were 0.08, 0.01 and 0.002 for 24Mg, 138Ba, and 238U, respectively. They were based on a 3σ criterion, where σ is the standard deviation of the mean blank count for each isotope. All the elemental concentrations in the outer shell layer were above the detection limits.

3. Results

3.1 Environmental parameters:

Around 10 m depth, the temperature varied from 2 °C in May to a maximum of 16 °C in early September and then decreased to 8 °C in November. At this depth, seawater temperature presents a classic seasonal cycle with cold water intrusions (Figure 4). During the first two weeks of September at 8 m and 12 m in Saint-Pierre Bay, temperature showed high-frequency variations with cold water incursions leading to 4°C (8m) to 6°C (12m) amplitudes (Figure 4). Along these two weeks, temperatures were 70% of the time above 12 °C (Figure 4).

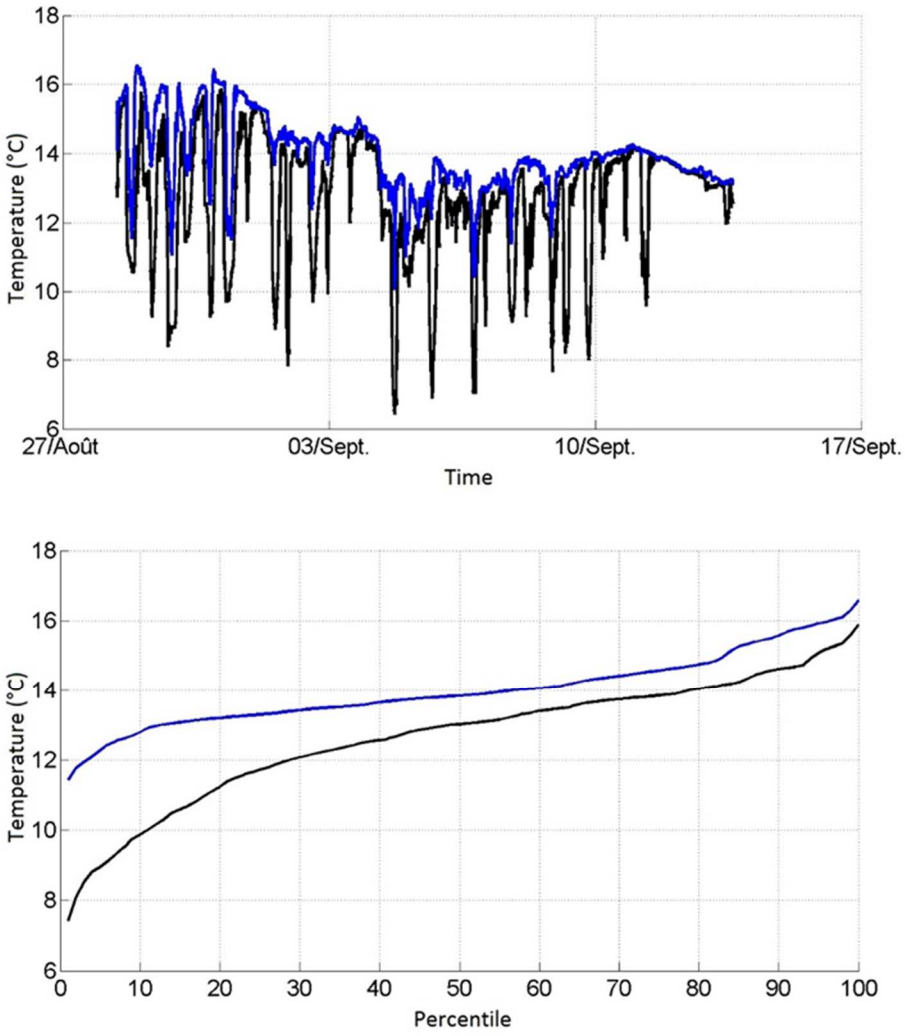

Figure 4: End of August and first two weeks of September 2017 time series of seawater temperatures at 8 m and 12m depth (blue and black) (top graphic). Percentile distribution of these temperatures at 8 m and 12m depth (blue and black).

At 30 m depth, the temperature annual profile was radically different (Figure 5). Seawater temperature baseline is mainly cold over the year, showing low seasonal amplitudes. However, during the stratified period, temperatures showed high-frequency variations whose amplitude increased with sea-surface temperature. During the first two weeks of September (Figure 5), oscillations were the largest in term of amplitude, reaching nearly 10°C. Along these two weeks, temperatures were 80% of the time below 8 °C (Figure 5).

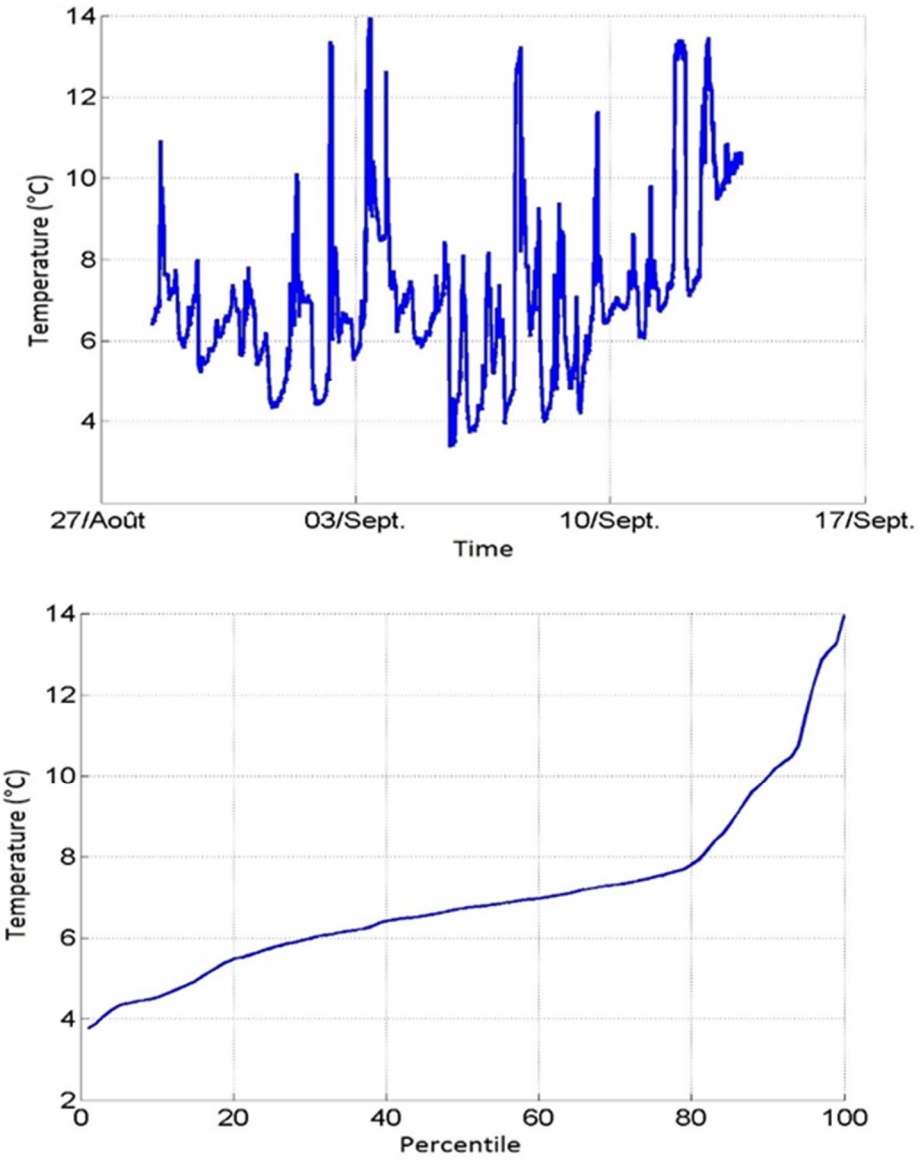

210

211 **Figure 5:** End of August and first two weeks of September 2017 time series of seawater
212 temperatures at 30m depth (top graphic). Percentile distribution of these temperatures
213 during these two weeks.

214

215 Monthly mean satellite chlorophyll *a* concentrations ranged from 0.46 to 1.22 $mg.m^{-3}$ (Figure
216 6). The annual time series-exhibited a background level around 0.7 $mg.m^{-3}$, with one major
217 peak in April - May 2015.

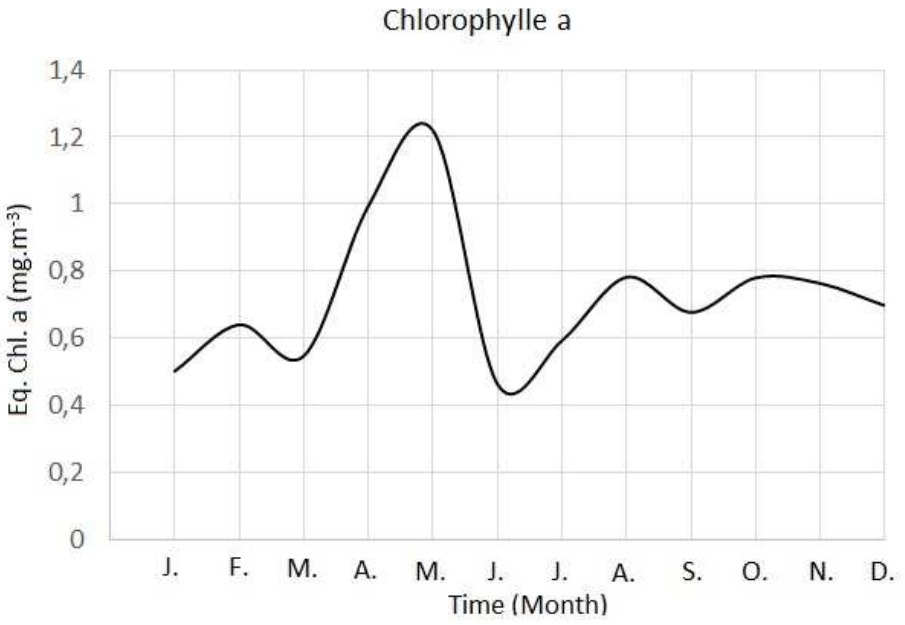

Figure 6: Monthly satellite equivalent chlorophyll a ($mg.m^{-3}$) measurements over the year 2015.

3.2 Ba/Ca ratio profiles in the shell carbonates

Outer shell layer Ba/Ca ratios ranged from 0.61 to 15.71 $\mu g.g^{-1}$ at 10 m and from 0.43 to 12.54 $\mu g.g^{-1}$ at 30 m (Figure 7). Both series have the same profile with one major peak occurring respectively 370 µm and 830 µm after the "winter 2014/2015" growth line. The main Ba/Ca peak covers 1370 and 2220 µm of shell at 10 and 30 m, respectively. A secondary smaller Ba/Ca peak occurred immediately after the first one, covering respectively 1230 and 1160 µm at 10 and 30 m. Ba/Ca baseline was the same for the two time-series (around 1.5 $\mu g.g^{-1}$).

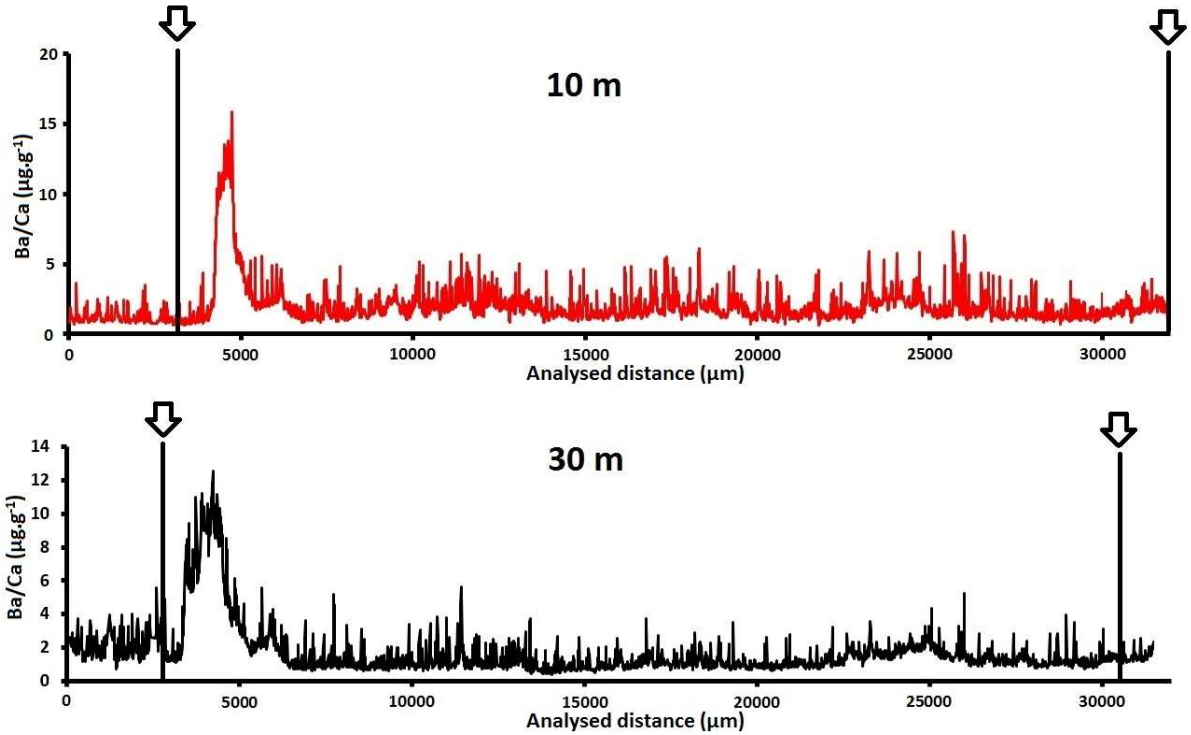

229

230 **Figure 7:** Ba/Ca (µg.g^{-1}) series at 10 m (red curve) and 30 m (black curve). Vertical lines
231 placed under the arrows indicate the position of winter shell growth lines.

232

233 ### 3.3 Mg/Ca ratio profiles

234 Outer shell layer Mg/Ca ratios ranged from 232 to 1408 µg.g^{-1} at 10 m and from 233 to 1495 µg.g^{-}
235 ^{1} at 30 m (Figure 8). At 10 m, Mg/Ca profile followed a sinusoidal pattern with stronger high
236 frequency variations between 15 000 and 25 000 µm (top and decreasing phase, Figure 8). At
237 30 m depth, the Mg/Ca profile was radically different with a globally flat profile between the
238 two growth lines and high frequency variations mainly between 15000 and 25000 µm (Figure
239 8).

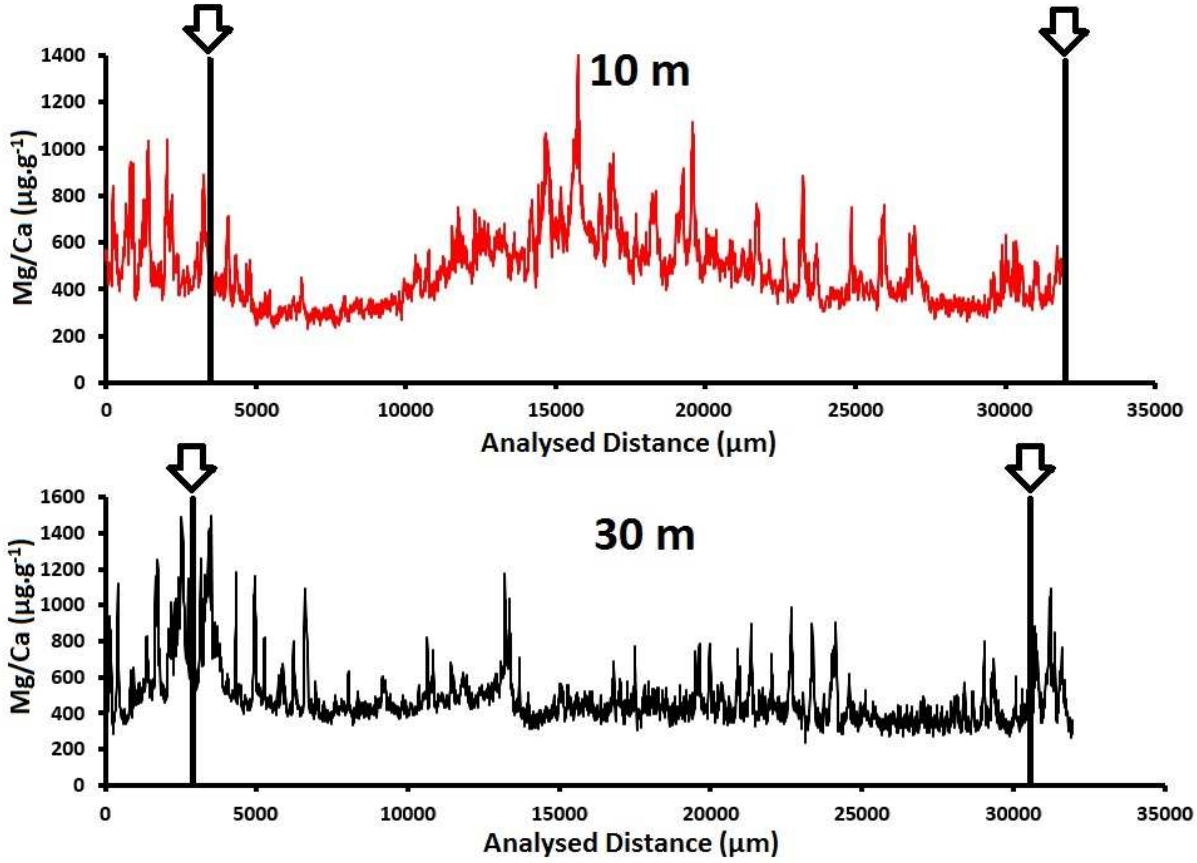

240

241 **Figure 8 :** Mg/Ca (µg.g^{-1}) series at 10 m (red curve) and 30 m (black curve). Vertical lines
242 placed under the arrows indicate the position of shell growth lines.

243

244 ### 3.4 U/Ca ratio profiles

245 Outer shell layer U/Ca ratios ranged from 0.003 to 0.16 µg.g^{-1} at 10 m and from 0.004 to 0.36 µg.g^{-1}
246 at 30 m (Figure 9). At 10 m depth, U/Ca time series had a relatively flat pattern with high-
247 frequency variations all along the profile. At 30 m depth, U/Ca profile was close to Mg/Ca one. So
248 we decided to compare those profiles in the next paragraph.

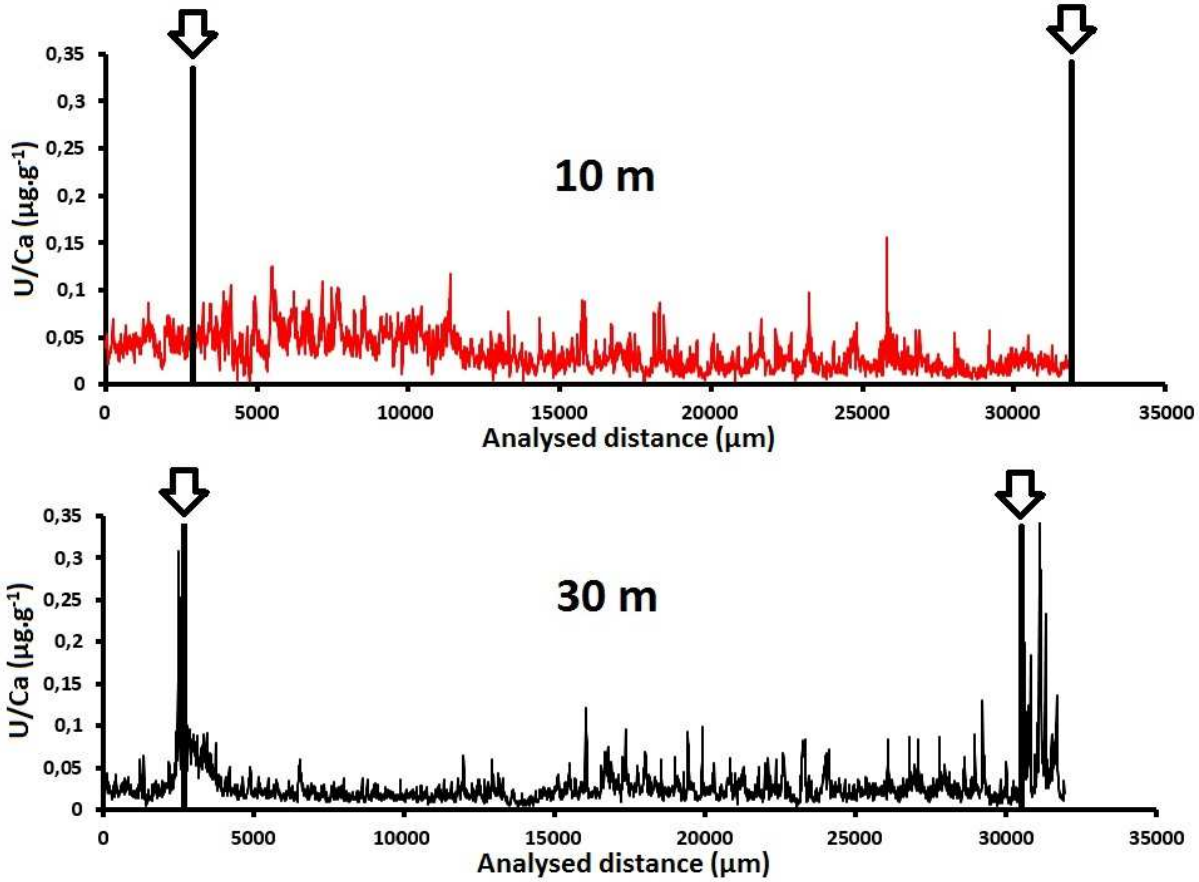

249

250 **Figure 9:** U/Ca (µg.g^{-1}) series at 10 m (red curve) and 30 m (black curve). Vertical lines placed
251 under the arrows indicate the position of shell growth lines.

252

253 **3.5 U/Ca and Mg/Ca comparison at 30m depth:**

254 At 30 m depth, U/Ca and Mg/Ca profiles presented a strong positive correlation (N = 3135, r =
255 0.62, $p < 0.001$) (Figure 10). A closer examination of this relationship on a shorter time window
256 (i.e. three high frequency cycles, between 22400 µm and 24250 µm) revealed an even stronger
257 correlation (N = 186, r = 0.77, $p < 0.001$).

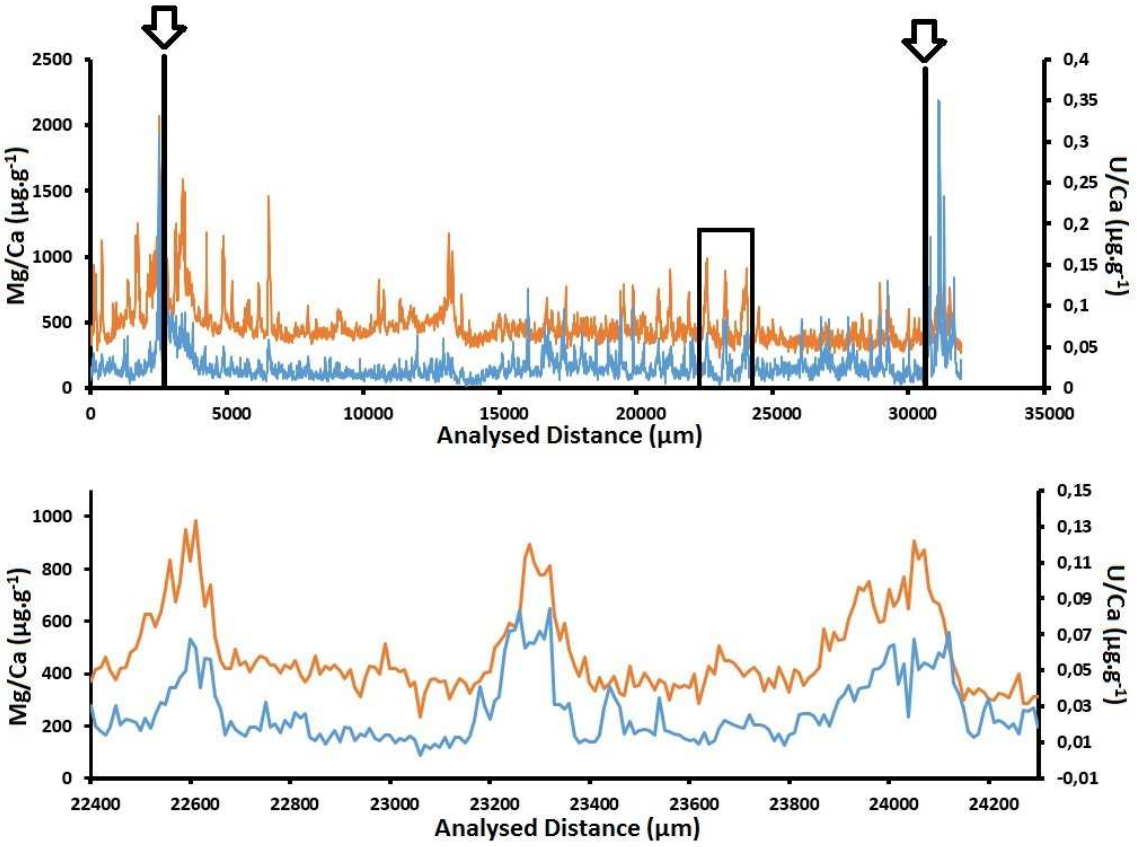

Figure 10: U/Ca (µg.g^{-1}) (blue curve) and Mg/Ca (µg.g^{-1}) (orange curve) series at 30 m. Vertical lines placed under the arrows indicate the position of shell growth lines. The graph bellow represents a close-up on three peaks (black box in the upper graph).

4. Discussion

This paper presents the first chemical analyses performed on *P. magellanicus* shells. Regarding the temporal resolution (25.82 h) of the environmental phenomena we wanted to track, it was necessary to develop a new analytical method. Our novel approach using ultra-high resolution fs-LA-ICPMS enables trace element analyses in bivalve shells with a 10-µm resolution. This study gave us first insights about *P. magellanicus* ability to record high-frequency environmental variations within is shell.

4.1 Barium

The high degree of similarity between the two Ba/Ca profiles suggests that the occurrence of Ba/Ca peaks was controlled by one or multiple common environmental factors. The pattern

of these two Ba/Ca profiles is similar to those observed in cross sections of other bivalve species (e.g., Gillikin *et al*., 2008; Stecher *et al*. 1996; Vander Putten *et al*., 2000). This confirms the hypothesis which suggests that the choice of analyzing the shell surface or the outer shell layer in cross sections do not have significant influence on Ba/Ca records in shells. In this section, we will discuss several hypotheses to explain temporal variability of Ba/Ca in *P. magellanicus* shell. Background levels of Ba/Ca time-series in bivalve shells have been suggested to record salinity variations (e.g. Gillikin *et al.*, 2006). There is generally a linear inverse relationship between seawater salinity and dissolved barium concentrations (Coffey *et al.*, 1997; Gillikin *et al.,* 2006). However, variability in seawater dissolved barium concentrations as a source for the Ba/Ca peaks in *P. magellanicus* from SPM is highly unlikely. Indeed, SPM islands, due to their offshore status, are not subjected to major riverine inputs and associated variations in salinity (Poitevin *et al.,* 2018). Salinity usually ranges from 31.3 to 32.2 PSU (see Figure 4 in Poitevin *et al.,* 2018) without a clear seasonal trend and, therefore, cannot explain Ba/Ca peaks measured in the shells. Many authors suggested a close relationship between these Ba/Ca peaks and phytoplankton blooms (e.g. Elliot *et al*., 2009; Lazareth *et al*., 2003; Stecher *et al*., 1996; Thébault *et al*., 2009; Vander Putten *et al.*, 2000). In our study, the high similarity of chlorophyll *a* concentration (Figure 6) and Ba/Ca (Figure 7) profiles strongly suggest a relationship between phytoplankton biomass and barium incorporation into *P. magellanicus* shells. Indeed, the occurrence of this bloom, in May 2015, seems to be consistent with the starting of *P. magellanicus* annual growth from other Canadian regions (Chute *et al*. 2012; Kleinman *et al*., 1996). Elevated levels of suspended barite ($BaSO_4$) have been suggested to be linked with oceanic diatoms primary productivity (Dehairs *et al*., 1991). Most of the barium released by diatoms after a bloom is labile and only a minor fraction eventually forms barite crystals (Ganeshram *et al.*, 2003). Therefore, if labile barium, either in phytoplankton or released into the dissolved phase, was the cause of the Ba/Ca peaks, these peaks should form near the end of the bloom or very shortly thereafter (Gillikin *et al.*, 2008). Considering the absence of daily growth lines in *P. magellanicus*, we cannot conclude about chlorophyll *a* and Ba/Ca peaks timing. Finally, the two Ba/Ca profiles exhibited a double peak, with a first large amplitude one and a smaller second peak. This observation has also been made in *P. maximus* Ba/Ca profiles (Gillikin *et al.*, 2008). One explanation for this double peak proposed in this study is based on Ganeshram e*t al.* (2003). They found that barite formation can take several weeks to reach its maximum after the

beginning of phytoplankton decay. Barite may be formed at the sediment surface and be ingested by *P. magellanicus* several weeks after the phytoplankton bloom ends.

These observations on Ba/Ca incorporation in *P. magellanicus* shell from SPM imply a real need for complementary information related to local *P. magellanicus* growth dynamics and physiology. It would also be crucial to get insights about the nature and the quantity of benthic and pelagic primary production over the year and along a bathymetric gradient.

4.2 Magnesium

In bivalve shells, the relationship between seawater temperature and Mg/Ca ratio is still subject to controversy. Some authors proposed that Mg/Ca ratios can be used to record water temperature (e.g., Bougeois *et al.,* 2014; Lazareth *et al*., 2003; Mouchi *et al.,* 2013; Surge and Lohmann, 2008; Ullmann *et al.,* 2013), while there are many reports of strong vital effects in bivalve shells for this element (e.g., Elliot *et al.,* 2009; Lorrain *et al.,* 2005, Wanamaker *et al.*, 2008,). In this study, we can hardly discuss the importance of vital effects on trace elements incorporation into *P. magellanicus* shell. Indeed, our analyses were only carried out on one year of growth (ontogenetic and calendar) and one individual per site. The only thing we can say about physiological control of Mg incorporation in *P. magellanicus* shell is based on Mg/Ca level. In this study, the mean Mg/Ca ratio (~500 $\mu g.g^{-1}$ corresponding to ~2$mmol.mol^{-1}$) of the calcitic outer shell layer of *P. magellanicus* corresponds to a low value compared to other calcitic mollusc shells (Lazareth *et al.*, 2007 and references therein). Given the absence of sclerochemical studies about trace element incorporation in *P. magellanicus* shells, we can only try to explain these low Mg concentrations relying on studies based on other calcitic bivalves with low Mg/Ca concentrations. For example, Lorens and Bender (1977) suggested that *Mytilus edulis* biologically regulates the amount of Mg entering the extrapallial fluid to produce low-Mg calcite. Perhaps a similar process occurs in *P. magellanicus*, suggesting a physiological control of Mg incorporation that could obscure Mg/Ca and seawater temperature relationship. This confirms the need for additional investigations on biomineralization, e.g. through experiments in controlled environments, in order to better understand trace elements incorporation in *P. magellanicus* shell. However, the shape of the two Mg/Ca profiles tend to highlight kind of a temperature control on magnesium

incorporation in our shells. At 10 m, the sinusoidal pattern of Mg/Ca ratio may reflect the seasonal seawater temperature annual cycle at 10 m depth. While at 30 m, the Mg/Ca profile presents a relatively flat baseline with high-frequency variations, which could mirror the seawater seasonal temperature trend, namely showing low seasonal amplitudes with high-frequency variations (Lazure *et al.,* 2018). Other studies also point to the non-systematic relationship between Mg/Ca ratio and SST. From a one year study of *M. edulis* growth, Vander Putten *et al.* (2000) observed a positive correlation between Mg/Ca and SST only during spring. Small-scale variations in Mg concentrations in *M. edulis* calcite have also been shown to derive from Mg being concentrated along the margins of calcite prisms (Rosenberg *et al.*, 2001). Indeed, the absence of interannual growth lines on the *P. magellanicus* shell is problematic to convert analysed distances in time. That is why enhance our knowledge on *P. magellanicus* growth dynamics along this bathymetric gradient in SPM would help us decipher physiological and environmental effects on trace element incorporation in *P. magellanicus* shell calcite. In addition, the lack of high frequency environmental data limits our ability to fully interpret our results and confirms the interest to set up a high frequency observatory along this bathymetric gradient.

4.3 Uranium

In our study, U/Ca and Mg/Ca profiles show a strong positive correlation in shells collected at 30 m (N=3135, r=0.62, p<0.001) (Fig. 10). However, this is not the case for the shallowest shells for which no significant correlation could be found. These results suggest that (i) environmental uranium availability for *P. magellanicus* are not the same between the two sites and/or (ii) that physiological differences between *P. magellanicus* from 10 m and 30 m sites could lead to differential incorporation of uranium in shells.

Since (i) we do not have information about *P. magellanicus* physiological differences between these two depths, and (ii) only few studies previously investigated U/Ca ratio as a potential paleo environmental proxy in bivalve shells (Frieder *et al.*, 2014; Gillikin and Dehairs, 2012; Zhao *et al.*, 2018), it seems difficult to draw conclusions about the kind of processes influencing uranium incorporation in *P. magellanicus* shells.

To our knowledge, U/Ca ratio as a paleo environmental proxy has been studied for the first time in mollusc shell by Gillikin and Dehairs (2012). In this study the authors tried to investigate U/Ca in *Saxidomus gigantea* shell as a potential acidification proxy and concluded that U/Ca may not reflect environmental variability and did not function as a paleo-pH proxy. More recently, Zhao *et al.* (2018) also found virtually unchanged U/Ca values in *Mya arenaria* shells with increasing seawater pCO_2 up to 2900 µatm. However, in the same study the authors found a significant increase in U/Ca ratio in shells with the increase in seawater pCO_2 at 6600 µatm. These findings reveal the existence of certain compensatory mechanisms by which this species may partially mitigate the impact of high environmental pCO_2 on shell formation through modifying the calcifying fluid chemistry to maintain its pH homeostasis (Zhao *et al.,* 2018). These conclusions lead us to consider *P. magellanicus* physiological responses induced by the repeated thermal variations occurring at the 31m site and their impact on the calcifying fluid pH of this species. Considering our study purpose and resolution, it seems difficult to conclude about U/Ca as a potential acidification proxy in *P. magellanicus* shell, especially as we do not have pH measurements on our study sites. Uranium-to-calcium ratios have also been suggested as a proxy for temperature in shallow water corals (e.g., Min *et al*., 1995; Shen and Dunbar, 1995) and in planktonic foraminiferal carbonates (e.g., Yu *et al*., 2008). In our study, the positive correlation between U/Ca and Mg/Ca profiles in the shell collected at 30 m would support this hypothesis. However, this correlation does not hold anymore at 10 m, suggesting that variations in uranium bioavailability differs between our two sites. Indeed, microorganisms have the ability to adsorb radionuclides/metals through extracellular binding involving physical adsorption, ion exchange, complexation and precipitation (Acharya *et al.*, 2009). They also sequester the metal ions by passive/active transport to the interior of the cell, followed by its accumulation. Microbial cells have been shown to reduce, oxidize, adsorb, accumulate and precipitate uranium (Fredrickson *et al.,* 1999; Macaskie *et al.,* 2000). So differences in microbial communities between the two sites, related to the nature of the habitat or to depth, could lead to changes in environmental uranium availability and finally to shell U/Ca ratios.

5. Conclusion

Our novel approach using ultra-high resolution fs-LA-ICPMS enables trace element analyses in bivalve shells with a 10-µm resolution. This study gave us first insights about *P. magellanicus* ability to record high-frequency environmental variations within is shell at a sub-hourly scale.

From an analytical point of view, it would be interesting to continue this study by applying this new analytical technique to more individuals. This would allow us to discuss about inter-individual variability within those two sites. Moreover, combining this approach with nano-SIMS $\delta^{18}O$ measurements (temperature proxy) would help us to get insights about the temperature control of Mg and U incorporation in shells.

In term of data interpretation, these results also confirm a real need for complementary information. Some of them should be related to *P. magellanicus* intra-annual growth dynamics. Indeed, in this study the absence of visible intra-annual growth lines visible on *P. magellanicus* shells hindered the temporal alignment of our microchemical data. Others must concern *P. magellanicus* physiological responses and their impacts on the calcifying fluid chemistry of this species. All these additional studies will require multiple high frequency environmental data continuously recorded at an individual scale within those two sites.

6. Acknowledgements

First, we thank the LEMAR (UMR 6539) Secretariat team (Anne-Sophie Podeur, Geneviève Cohat, and Yves Larsonneur) for their invaluable assistance during the administrative preparation of the analytical trip associated with this work in Pau. We also thank Gaëlle Barbotin for her help during fs-LA-ICPMS measurements in Pau. This work was supported by the EC2CO program MATISSE of the CNRS INSU, the Cluster of Excellence LabexMER, and the LIA BeBEST CNRS INEE. This research was carried out as part of the Ph.D. thesis of Pierre Poitevin for the University of Western Brittany with a French Ministry of Higher Education and Research grant. This manuscript greatly benefited from very useful comments made by the reviewers.

7. References

Acharya C, Joseph D, Apte SK (2009) Uranium sequestration by a marine cyanobacterium *Synechococcus elongatus* strain BDU/75042. *Bioressource Technology*, **100**, 2176-2181.

Ballesta-Artero I, Witbaard R, Carroll ML, Van der Meer J (2017) Environmental factors regulating gaping activity of the bivalve *Arctica islandica* in Northern Norway. *Marine Biology*, **164 (5)**, 116.

Barats A, Amouroux D, Pecheyran C, Chauvaud L, Donard OFX (2007) High-Frequency Archives of Manganese Inputs To Coastal Waters (Bay of Seine, France) Resolved by the LA ICPMS Analysis of Calcitic Growth Layers along Scallop Shells (*Pecten maximus*). *Environmental Science & Technology*, **42 (1**), 86-92.

Bougeois L, de Rafélis M, Reichart GJ, de Nooijer LJ, Nicollin F, Dupont-Nivet G (2014) A high resolution study of trace elements and stable isotopes in oyster shells to estimate Central Asian Middle Eocene seasonality. *Chemical Geology*, **363**, 200-212.

Butler PG, Richardson CA, Scourse JD, et al. (2010) Marine climate in the Irish Sea: analysis of a 489-year marine master chronology derived from growth increments in the shell of the clam *Arctica islandica*. *Quaternary Science Reviews*, **29**, 1614–1632.

Carré M, Bentaleb I, Bruguier O, Ordinola E, Barrett NT, Fontugne M (2006) Calcification rate influence on trace element concentrations in aragonitic bivalve shells: Evidences and mechanisms. *Geochimica et Cosmochimica Acta*, **70**, 4906-4920.

Chauvaud L, Thouzeau G, Paulet YM (1998) Effects of environmental factors on the daily growth rate, *Journal of Experimental Marine Biology and Ecology*, **227**, 83–111.

Chung GS, Swart PK (1990) The concentration of uranium in freshwater vadose and phreatic cements in a Holocene ooid cay; a method of identifying ancient water tables. *Journal of Sedimentary Research*, **60**, 735-746.

Chute AS, Wainright SC, Hart DR (2012) Timing of shell ring formation and patterns of shell growth in the sea scallop *Placopecten magellanicus* based on stable oxygen isotopes. *Journal of Shellfish Research*, **31**, 649- 662.

Coffey M, Dehairs F, Collette O, Luther G, Church T, Jickells T (1997) The behaviour of dissolved barium in estuaries. *Estuarine, Coastal and Shelf Science*, **45**, 113-121.

Dehairs F, Stroobants N., Goeyens L (1991) Suspended barite as a tracer of biological activity in the Southern Ocean. *Marine Chemistry*, **35**, 399–410.

448 Elliot M, Welsh K, Chilcott C, McCulloch M, Chappell J, Ayling B (2009) Profiles of trace
449 elements and stable isotopes derived from giant long-lived *Tridacna gigas* bivalves: Potential
450 applications in paleoclimate studies. *Palaeogeography, Palaeoclimatology, Palaeoecology*,
451 **280**, 132-142.

452 Fredrickson JK, Kostandarithes HM, Li SW, Plymale AE, Daly MJ (1999) Reduction of Fe(III),
453 Cr(VI), U(VI) and Te(VII) by *Deinococcus radiodurans* R1. *Applied Environmental Microbiology*,
454 **66**, 2006–2011.

455 Freitas PS, Clarke LJ, Kennedy H, Richardson CA (2008) Inter- and intra-specimen variability
456 masks reliable temperature control on shell Mg/Ca ratios in laboratory- and field-cultured
457 *Mytilus edulis* and *Pecten maximus* (bivalvia). *Biogeosciences*, **5**, 1245-1258.

458 Freitas PS, Clarke LJ, Kennedy H, Richardson CA (2009). Ion microprobe assessment of the
459 heterogeneity of Mg/Ca, Sr/Ca and Mn/Ca ratios in *Pecten maximus* and *Mytilus edulis*
460 (bivalvia) shell calcite precipitated at constant temperature. *Biogeosciences*, **6**, 1209-1227.

461 Freitas PS, Clarke LJ, Kennedy H, Richardson CA (2016) Manganese in the shell of the bivalve
462 *Mytilus edulis*: Seawater Mn or physiological control? *Geochimica et Cosmochimica Acta*, **194**,
463 266-278.

464 Frieder CA, Gonzalez JP, Levin LA (2014) Uranium in Larval Shells As a Barometer of Molluscan
465 Ocean Acidification Exposure. *Environmental Science & Technology*, **48 (11)**, 6401-
466 6408.Ganeshram RS, Francois R, Commeau J, Brown-Leger SL (2003) An experimental
467 investigation of barite formation in seawater. *Geochimica et Cosmochimica Acta*, **67**, 2599-
468 2605.

469 Gillikin D, Dehairs F, Lorrain A, Steenmans D, Baeyens W, Andre L (2006) Barium uptake into
470 the shells of the common mussel (*Mytilus edulis*) and the potential for estuarine paleo-
471 chemistry reconstruction. *Geochimica et Cosmochimica Acta*, **70**, 395-407.

472 Gillikin D, Lorrain A, Paulet YM, Andre L, Dehairs F (2008) Synchronous barium peaks in high-
473 resolution profiles of calcite and aragonite marine bivalve shells. *Geo-Marine Letters*, **28**, 351-
474 358.

475 Gillikin D, Dehairs F (2012) Uranium in aragonitic marine bivalve shells, *Palaeogeography,*
476 *Palaeoclimatology, Palaeoecology*, **373**, doi: 10.1016/j.palaeo.2012.02.028.

Kitano Y, Oomori T (1971) The coprecipitation of uranium with calcium carbonate. *Journal of the Oceanographic Society of. Japan*, **27**, 34–42.

Klein R, Lohmann K, Thayer C (1996) Sr/Ca and C-13/C-12 ratios in skeletal calcite of *Mytilus trossulus*: Covariation with metabolic rate, salinity, and carbon isotopic composition of seawater. *Geochimica et Cosmochimica Acta*, **60**, 4207-4221.

Kleinman S, Hatcher BG, Scheibling RE, Taylor LH, Hennigar AW (1996) Shell and tissue growth of juvenile sea scallops (*Placopecten magellanicus*) in suspended and bottom culture in Lunenburg Bay, Nova Scotia. *Aquaculture*, **142**, 75–97.

Langmuir D (1978) Uranium mineral-solution equilibria. *Geochimica et Cosmochimica Acta*, **42**, 547–569.

Lazareth CE, Vander Putten E, André L, Dehairs F (2003) High-resolution trace element profiles in shells of the mangrove bivalve *Isognomon ephippium*: a record of environmental spatio-temporal variations? *Estuarine, Coastal and Shelf Science*, **57**, 1103–1114.

Lazareth CE, Guzman N, Poitrasson F, Candaudap F, Ortlieb L (2007) Nyctemeral variations of magnesium intake in the calcitic layer of a Chilean mollusk shell (*Concholepas concholepas*, Gastropoda), *Geochimica et Cosmochimica Acta*, **71**, 5369-5383.

Lazareth CE, Le Cornec F, Candaudap F, Freydier R (2013) Trace element heterogeneity along isochronous growth layers in bivalve shell: Consequences for environmental reconstruction. *Palaeogeography, Palaeoclimatology, Palaeoecology*, **373**, 39-49.

Lazure P., Le Cann B., Bezaud M. (2018) Large diurnal bottom temperature oscillations around the Saint Pierre and Miquelon archipelago. *Scientific Reports*, **8**, Article number: 13882.

Lorens R, Bender M (1977) Physiological Exclusion of Magnesium from *Mytilus edulis* Calcite. *Nature*, **269**, 793-794.

Lorrain A, Gillikin D, Paulet YM, Chauvaud L, Le Mercier A, Navez J, André L (2005) Strong kinetic effects on Sr/Ca ratios in the calcitic bivalve *Pecten maximus*. *Geology*, **33 (12)**, 965-968.

Macaskie LE, Bonthrone KM, Yong P, Goddard D (2000) Enzymatically-mediated bioprecipitation of uranium by a *Citrobacter sp.*: a concerted role for extracellular

505 lipopolysaccharides and associated phosphatase in biomineral formation. *Microbiology*, **146**,
506 1855–1867.

507 Marali S, Schöne BR (2015) Oceanographic control on shell growth of *Arctica islandica*
508 (Bivalvia) in surface waters of Northeast Iceland—implications for paleoclimate
509 reconstructions. *Palaeogeography, Palaeoclimatology, Palaeoecology*, **420**, 138-149.

510 Min GR, Edwards RL, Taylor FW, Recy J, Gallup CD, Beck JW (1995) Annual cycles of U/Ca in
511 coral skeletons and U/Ca thermometry. *Geochimica et Cosmochimica Acta*, **59**, 2025-2042.

512 Mouchi V, de Rafélis M, Lartaud F, Fialin M, Verrecchia E (2013) Chemical labelling of oyster
513 shells used for time-calibrated high-resolution Mg/Ca ratios: a tool for estimation of past
514 seasonal temperature variations*. Palaeogeography. Palaeoclimatology. Palaeoecology*, **373**,
515 66–74.

516 Poitevin P, Thébault J, Schöne BR, Jolivet A, Lazure P, Chauvaud L (2018) Ligament, hinge, and
517 shell cross-sections of the Atlantic surfclam (*Spisula solidissima*): Promising marine
518 environmental archives in NE North America. *Plos One*, **13(6)**, e0199212.

519 Rosenberg GD, Hughes WW, Parker DL, Ray BD (2001) The geometry of bivalve shell chemistry
520 and mantle metabolism, *American Malacological Bulletin*, **16**, 251–261.

521 Schöne BR, Radermacher P, Zhang Z, Jacob DE (2013) Crystal fabrics and element impurities
522 (Sr/Ca, Mg/Ca, and Ba/Ca) in shells of *Arctica islandica*-Implications for paleoclimate
523 reconstructions. *Palaeogeography, Palaeoclimatology, Palaeoecology*, **373**, 50-59.

524 Shen GT, Dunbar RB (1995) Environmental controls on uranium in reef corals. *Geochimica et*
525 *Cosmochimica Acta*, **59**, 2009-2024

526 Shirai K, Schöne BR, Miyaji T, Radarmacher P, Krause RA Jr., Tanabe K (2014) Assessment of
527 the mechanism of elemental incorporation into bivalve shells (*Arctica islandica*) based on
528 elemental distribution at the microstructural scale. *Geochimica et Cosmochimica Acta*, **126**,
529 307-320.

530 Stecher HA, Krantz DE, Lord CJ, Luther GW, Bock KW (1996) Profiles of strontium and barium
531 in *Mercenaria mercenaria* and *Spisula solidissima* shells. *Geochimica et Cosmochimica Acta*,
532 **60 (18)**, 3445-3456.

533 Stecher HA, Kogut MB (1999) Rapid Barium removal in the Delaware estuary. *Geochimica et*
534 *Cosmochimica Acta*, **63**, 1003-10012.

535 Surge D, Lohmann KC (2008) Evaluating Mg/Ca ratios as a temperature proxy in the estuarine
536 oyster, *Crassostrea virginica*. *Journal of Geophysical Research*, **113**, G02001.

537 Thébault J, Chauvaud L, L'Helguen S, Clavier J, Barats A, Jacquet S, Pecheyran C, Amouroux D
538 (2009). Barium and molybdenum records in bivalve shells: Geochemical proxies for
539 phytoplankton dynamics in coastal environments? *Limnology and Oceanography*, **54**, 1002-
540 1014.

541 Ullmann CV, Böhm F, Rickaby REM, Wiechert U, Korte C (2013). The Giant Pacific Oyster
542 (*Crassostrea gigas*) as a modern analog for fossil ostreoids: isotopic (Ca, O, C) and elemental
543 (Mg/Ca, Sr/Ca, Mn/Ca) proxies. *Geochemistry, Geophysics, Geosystems*, **14**, 4109–4120.

544 Vander Putten, E, Dehairs F, Keppens E, Baeyens W (2000) High resolution distribution of trace
545 elements in the calcite shell layer of modern *Mytilus edulis*: Environmental and biological
546 controls. *Geochimica et Cosmochimica Acta*, **64**, 997-1011.

547 Wanamaker AD, Kreutz KJ, Wilson T, Borns HW, Introne DS, Feindel S (2008) Experimentally
548 determined Mg/Ca and Sr/Ca ratios in juvenile bivalve calcite for *Mytilus edulis*: implications
549 for paleotemperature reconstructions. *Geo-Marine Letters*, **28**, 359-368.

550 Warter V, Müller W (2017) Daily growth and tidal rhythms in Miocene and modern giant clams
551 revealed via ultra-high resolution LA-ICPMS analysis - A novel methodological approach
552 towards improved sclerochemistry. *Palaeogeography, Palaeoclimatology, Palaeoecology*,
553 **465**, 362-375.

554 Witbaard R, Duineveld GCA, DeWilde PAWJ (1997) A long-term growth record derived from
555 *Arctica islandica* (Mollusca, Bivalvia) from the Fladen Ground (northern North Sea). *Journal of*
556 *the Marine Biological Association of the United Kingdom*, **77 (3)**, 801–816.

557 Yu J, Elderfield H, Jin Z, Booth L (2008) A strong temperature effect on U/Ca in planktonic
558 foraminiferal carbonates. *Geochimica et Cosmochimica Acta*, **72**, 4988–5000.

559 Zhao L, Milano S, Walliser EO, Schöne BR (2018) Bivalve shell formation in a naturally CO2-
560 enriched habitat: Unraveling the resilience mechanisms from elemental signatures.
561 *Chemosphere*, **203**, 132-138.